

Research Article

Wideband Omnidirectional Slotted-Waveguide Antenna Array Based on Trapezoidal Slots

Hugo Rodrigues Dias Filgueiras ¹, James R. Kelly,² Pei Xiao ³, I. F. da Costa ⁴,
and Arismar Cerqueira Sodré Jr. ¹

¹Laboratory WOCA (Wireless and Optical Convergent Access), National Institute of Telecommunications, Santa Rita do Sapucaí, MG 37540-000, Brazil

²Queen Mary University of London, Mile End Rd, London E1 4NS, UK

³ICS/5GIC, The University of Surrey, Stag Hill Campus, Guildford GU2 7XH, UK

⁴ESSS, São Paulo 04552-906, Brazil

Correspondence should be addressed to Hugo Rodrigues Dias Filgueiras; hugorodrigues@get.inatel.br and Arismar Cerqueira Sodré Jr.; arismar@inatel.br

Received 4 April 2019; Accepted 8 August 2019; Published 13 October 2019

Academic Editor: Yuan Yao

Copyright © 2019 Hugo Rodrigues Dias Filgueiras et al. This is an open access article distributed under the Creative Commons Attribution License, which permits unrestricted use, distribution, and reproduction in any medium, provided the original work is properly cited.

This manuscript presents a novel approach for designing wideband omnidirectional slotted-waveguide antenna arrays, which is based on trapezoidal-shaped slots with two different electrical lengths, as well as a twisted distribution of slot groups along the array longitudinal axis. The trapezoidal section is formed by gradually increasing the slot length between the waveguide interior and exterior surfaces. In this way, a smoother impedance transition between waveguide and air is provided in order to enhance the array operating bandwidth. In addition, we propose a twisting technique, responsible to improve the omnidirectional pattern, by means of reducing the gain ripple in the azimuth plane. Experimental results demonstrate 1.09 GHz bandwidth centered at 24 GHz (4.54% fractional bandwidth), gain up to 14.71 dBi over the operating bandwidth, and only 2.7 dB gain variation in the azimuth plane. The proposed antenna array and its enabling techniques present themselves as promising solutions for mm-wave application, including 5G enhanced mobile broadband (eMBB) communications.

1. Introduction

Real-time low-latency communications, video streaming, and the so-called internet of things (IoT) have continually increased the network throughput demand [1, 2], which expedites the need for an entirely new concept for wireless systems. The fifth generation of mobile communication (5G) is a promising solution focused on enabling users, objects, data, and applications to be connected to an intelligent network environment [1, 2]. The main and most-probable 5G scenarios are follows [3]: enhanced mobile broadband (eMBB) communications; massive machine-type communications (mMTC); ultrareliable low latency (URLL) applications; and remote and rural areas.

Particularly, enhanced mobile broadband applications require wide bandwidth. However, the sub-6 GHz frequency

spectrum is overloaded with the current wireless standards. A potential solution is migrating eMBB to the millimeter-wave (mm-wave) frequency range, which is unexploited worldwide and allows the use of hundreds of MHz bandwidth [4]. On the other hand, the use of mm-waves implies new challenges, such as high propagation losses and blockage due to walls and obstacles [4–6]. As a result, it becomes necessary to deploy more base stations, performing as small range cells, picocells and femtocells. High directive antennas and antenna arrays are desired to compensate the wireless system high losses [2, 7].

Multiple-input multiple-output (MIMO) techniques rely on using multiple radiating elements for increasing the system spectral efficiency based on different approaches [7], including spatial multiplexing (SM) and beamforming (BF). SM consists of simultaneously transmitting multiple data

streams using different channels and spatially dislocated antennas, with the aim of enhancing the channel capacity and system throughput. Beamforming is the association of multiple resonant elements for creating a unique directive beam with or without beamsteering capacity. BF is typically applied to provide signal-to-noise increment. Both techniques can be used in either the transmitter or receiver side.

Most of the mm-wave antenna arrays for MIMO from the literature are based on patch antennas [7, 8]. They are composed of planar structures and a feeding network based on multiple RF chains for enabling to manage the amplitude and/or phase among the array elements to achieve beamsteering and/or beamforming capacity. Their major design challenge is the feeding network complexity at higher frequencies. On the other hand, for achieving gain increment, slotted-waveguide antenna arrays (SWAAs) present themselves as a promising solution and their elements simply fed by a unique coaxial-waveguide transition [9–12]. SWAAs consist of slots milled into waveguide walls, with the purpose of interrupting the current flow for enabling radiofrequency radiation. Each slot acts as an isolated antenna, and consequently, a waveguide with a plurality of slots works as an antenna array.

SWAAs provide high gain and are high-power handling, thus are typically applied to radar systems operating at microwaves and mm-waves [13, 14]. Other applications include satellite television reception [15], land mines activation [16], and pressure sensors [17]. Our research group has recently proposed novel SWAAs for 5G networks [18–21]. For instance, we have introduced a concept of a rectangular dual-band SWAA with sectorial coverage in the 28 and 38 GHz bands [18]. It was based on slots with two different electrical lengths, one for each frequency band. Moreover, the first optically controlled antenna array for mm-wave from literature was reported in [19]. Finally, a mechanically reconfigurable SWAA operating at 27 GHz has been proposed and properly validated in [20].

This work is regarding a novel approach for designing wideband omnidirectional SWAAs based on trapezoidal-shaped slots with two different electrical lengths. The manuscript is structured in four sections. Section 2 presents the new structure and its numerical results, whereas its prototype and experimental results are reported in Section 3. Lastly, conclusions and future works are outlined in Section 4.

2. Novel SWAA Design

The trapezoidal-shaped slots, claimed and patented in [22], are illustrated in Figure 1. Each slot is formed by cutting a trapezoidal prism-shaped hole into the waveguide wall. The slanted sides of the trapezoidal prism are orientated along the radial direction. As a consequence, a smoother transition between the waveguide and air is created by progressively changing the slot radiating impedance. Such a technique can be compared to tapered line transitions and biconical antennas, in which their resistance and reactance variations became less severe as the cone angle increases [23]. Two more additional variables must be taken into consideration

when trapezoidal slots are used: the waveguide wall thickness (t) and the slot outer length ($l_{\text{out_slot1}}$). We have used groups of slots with two different electrical lengths for obtaining two resonances and expanding the array bandwidth, as demonstrated in [18], giving rise to a third additional variable, which is the length of each slot from the second group ($l_{\text{out_slot2}}$) in our particular design.

The novel slotted-waveguide antenna array is based on trapezoidal slots milled into a circular waveguide, as presented in Figure 2. The transversal magnetic (TM_{01}) mode had been chosen to excite the array for providing a uniform electric field distribution across the waveguide transverse section, giving rise to an omnidirectional pattern in the azimuth plane. The propagating mode has been ensured by using a K -connector (2.92 mm) with the inner conductor entering normally to the waveguide transverse section as presented in Figure 2.

A standard WC44 waveguide has been used to excite the antenna array, which has been milled to a second standard waveguide (WC69). We have chosen the WC44 for exciting the array because of its cutoff frequency, which is 20.6 GHz. In this way, we could ensure that only the desired propagating mode was used to excite the antenna array. The level of ripple in the omnidirectional radiation pattern (azimuthal plane) is proportional to the number of slots distributed around the circumference of the waveguide. The WC69 waveguide has been used as a radiating structure for reducing the cutoff frequency. As a consequence, the reduction in the guided wavelength implies in a large number of slots around its circumference. In addition, the waveguide has been filled with low loss Teflon ($\text{tg}\delta = 0.001$) for further reducing the guided wavelength and minimizing loss due to power dissipation. Details on the proposed SWAA feeding structure, including the transition and dielectric cone heights ($h_{\text{transition}}$ and h_{cone}), are illustrated in Figure 2. These dimensions are very critical for the array impedance matching since they are responsible to generate a smooth transition between the feeder and the waveguide. Their final values have been obtained by numerical sweeps in ANSYS HFSS.

The proposed antenna array has been designed to operate in the 24 GHz band, which has been considered a potential candidate for 5G networks in Brazil. The slot length (l_{slot}) was set to one half of the guided wavelength (λ_g) [23], by considering the WC69 cutoff frequency ($f_c = 9.07$ GHz) for TM_{01} mode and Teflon permittivity ($\epsilon_r = 2.1$). However, other propagating modes may be guided into the antenna array structure and slots themselves, including TM_{11} , TM_{21} , TM_{02} , and TM_{31} , because of their cutoff frequencies, which are 14.45, 19.36, 20.81, and 24.05 GHz, respectively. This feature might cause phase disturbance inside the waveguide and, consequently, may degrade the array overall radiation pattern performance. One can overcome such an issue by properly managing the slot spacing (d_{slot}) and optimizing its height (h_{slot}) in order to obtain the correct phase distribution among the slots for ensuring a uniformly distributed electric field across the waveguide transverse section, as desired. In other words, the antenna array design will differ from that presented in [10–12], since the distance between consecutive

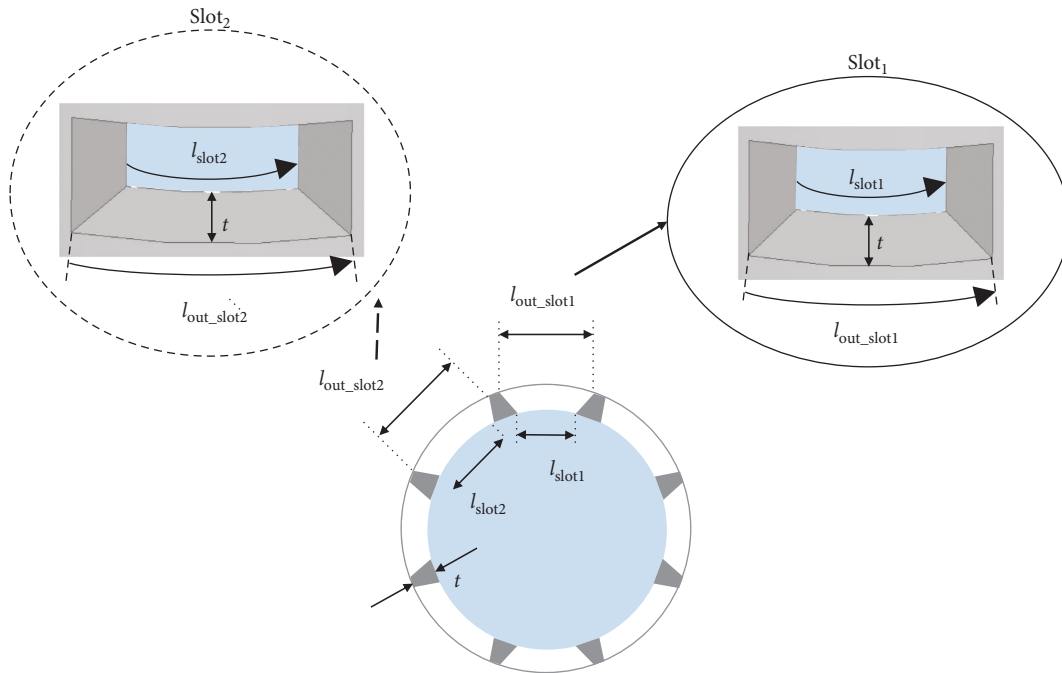


FIGURE 1: Trapezoidal-shaped slots details.

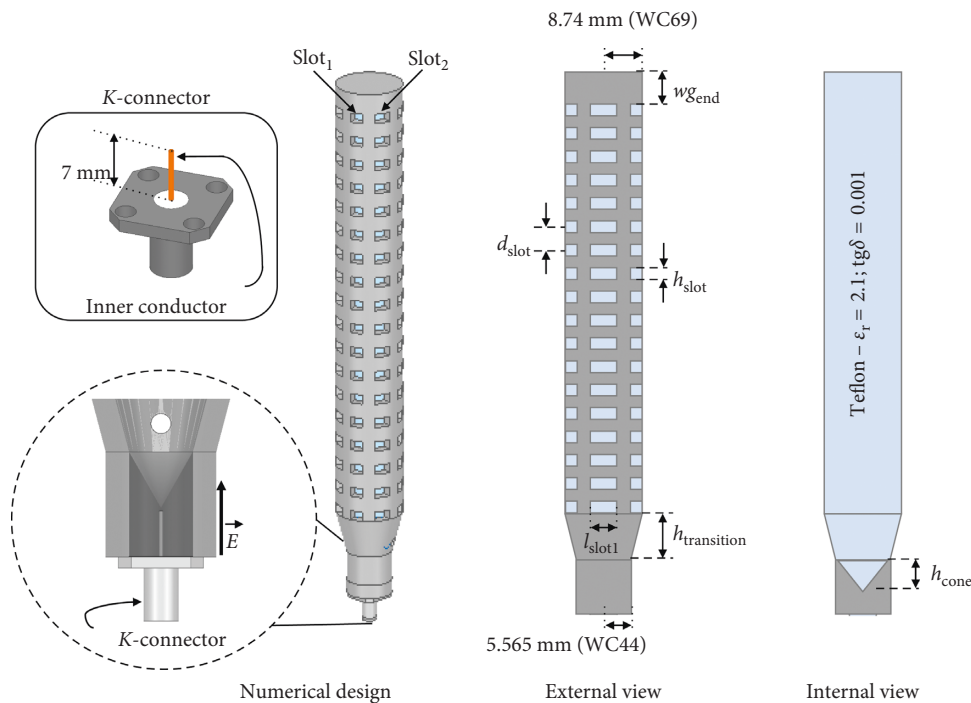


FIGURE 2: Novel SWAA design based on trapezoidal-shaped slots with two different electrical lengths.

slots is not exactly one-half of the guided wavelength. This parameter was obtained by parametric analysis as a function of gain and side lobe level (SLL).

As a resonant antenna array, the distance between the waveguide end wall and last slot center was designed as a quarter of the guided wavelength. Basically, the parameter $w_{g_{end}}$ has been calculated to ensure an electric field null at the waveguide end wall, with the aim of constructively

reflecting the nonradiated energy. One can mathematically calculate $w_{g_{end}}$ as $0.25(2p + 1)\lambda_g - 0.5h_{slot}$, where p is an integer number [23]. The antenna array final dimensions were $l_{slot1} = 4.4$ mm, $d_{slot} = 7.15$ mm, $h_{slot} = 3.5$ mm, $w_{g_{end}} = 4.02$ mm, $h_{transition} = 15$ mm, and $h_{cone} = 8.77$ mm.

Conventional SWAAs are typically narrowband [9, 23, 24]. Figure 3 presents a frequency response comparison among two conventional SWAAs and one based on

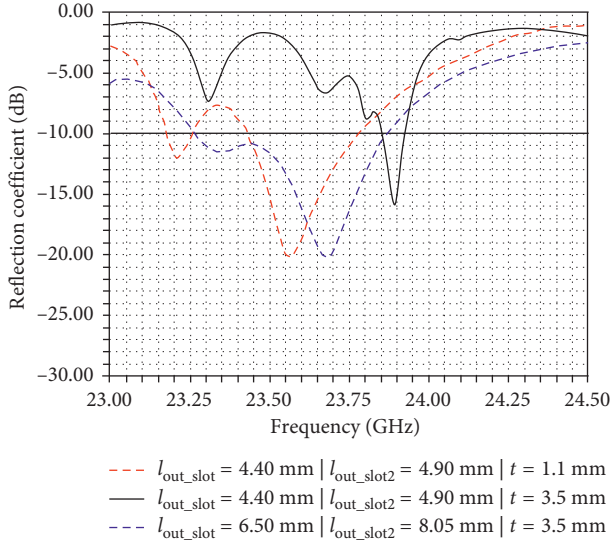


FIGURE 3: Reflection coefficient comparison: dashed-red and solid-black lines are conventional SWAAs with 1 mm and 3.5 mm waveguides thickness, respectively; the dotted-blue line is an SWAA based on trapezoidal-shaped slots with waveguide thickness equal to 3.5 mm.

trapezoidal-shaped slots, as a function of their main design parameters, namely, the waveguide wall thickness and length of slots 1 and 2. The waveguide thickness has been increased from 1.1 to 3.5 mm for allowing the trapezoidal-shaped slot approach implementation. The conventional SWAA ($l_{\text{out_slot}} = 4.4 \text{ mm}$, $l_{\text{out_slot2}} = 4.9 \text{ mm}$, and $t = 1.1 \text{ mm}$) yields a 350 MHz bandwidth, which corresponds to 1.48% fractional bandwidth at 24 GHz for reflection coefficient lower or equal to -10 dB . When its wall thickness is set to 3.5 mm, the bandwidth is reduced to 70 MHz (0.29%). On the other hand, by replacing the rectangular slots with trapezoidal-shaped ones, one can increment the bandwidth by 71%, giving rise to 600 MHz bandwidth (2.55%).

Figure 4 reports the influence and demonstrates the effectiveness of applying trapezoidal-shaped slots for enhancing the SWAA bandwidth. The Smith charts obtained for the novel technique are much closer to chart center over the entire analyzed frequency range (from 23.0 to 24.5 GHz) than those of the conventional SWAA, which is based on rectangular slots. For instance, the input impedance of the rectangular (solid black curve) and trapezoidal-shaped (dotted blue curve) slots at 23.7 GHz are $Z = 19.98 + i17.83 \Omega$ and $Z = 60.50 + i4.1 \Omega$, respectively. Therefore, a clear and significant improvement in both real and imaginary parts of the input impedance is observed.

The next step in the antenna development was focused on improving the omnidirectional radiation pattern, by applying a technique based on a twisted distribution of slot groups along the array longitudinal axis, as we have very recently proposed in [21]. Specifically, an angular displacement (α) has been introduced between consecutive rings of slots, as defined in Figure 5(a). The twisting effect significantly reduces the gain ripple in the azimuth plane, as proved in Figure 5(b), without interfering in the input

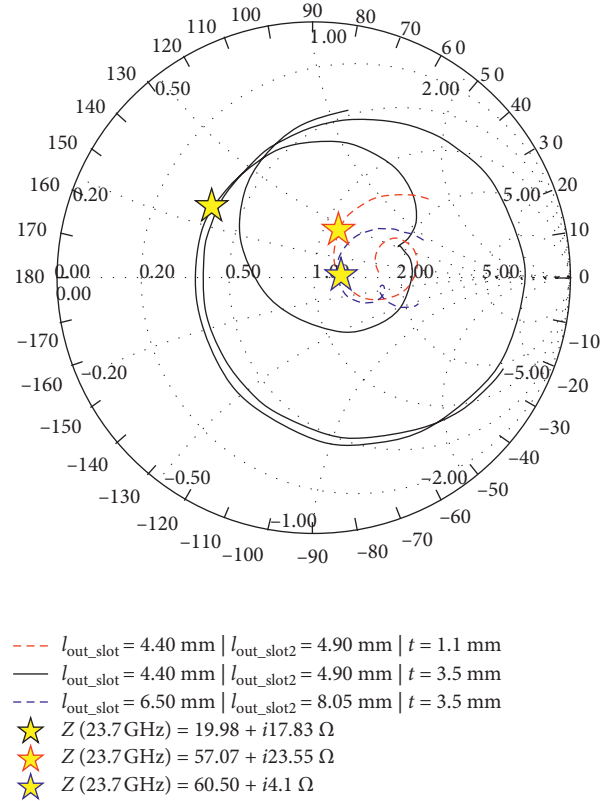


FIGURE 4: Smith chart analysis from 23.2 to 24 GHz to demonstrate the effectiveness of the trapezoidal-shaped slots.

impedance matching. The gain variation in the azimuth plane ranges from 40 to 1.7 dB, as α is varied from 0° to 22.5° , which results in a more uniform omnidirectional coverage. Table 1 presents the twisted SWAA final dimensions.

3. Experimental Results

This section is concerning the experimental results of the novel slotted-waveguide antenna array prototype (Figure 6) based on trapezoidal-shaped slots with two different lengths and distributed in a twisted way along its longitudinal axis. Initially, a comparison between the reflection coefficient numerical and experimental results has been realized, as reported in Figure 7. The measured -10 dB reflection coefficient bandwidth was 1.09 GHz centered at 24.15 GHz, which corresponds to a fractional bandwidth of 4.52% and results in an enhancement of three times when compared to the conventional SWAA. One can observe an acceptable agreement between simulation and experiment up to 23.8 GHz; above this frequency, there are some differences most notably at the upper cutoff frequency, implying in a wider measured bandwidth. This discrepancy might be explained by imprecisions in the manufacturing process, which were not considered in the numerical simulations.

The SWAA radiation pattern has been measured in steps of 1° , by using an analog signal generator, a 25 dBi gain horn antenna as a reference and a spectrum analyzer. We have conducted the measurements at 23.6, 24.15, and 24.7 GHz, which represent the lower, central, and higher frequencies of

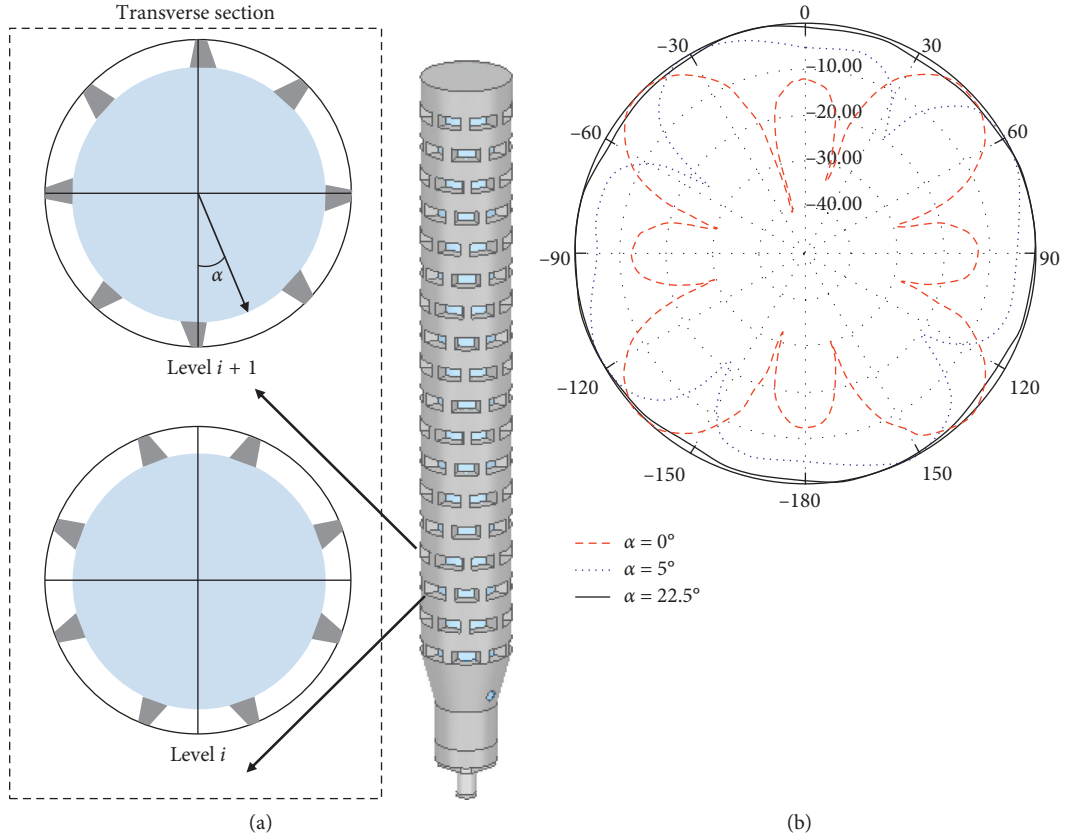


FIGURE 5: Twisting technique for enhancing the omnidirectional coverage. (a) Angle displacement definition. (b) Radiation pattern in the azimuth plane at 23.7 GHz for distinct values of α .

TABLE 1: Twisted SWAA final dimensions.

Variable	Value (mm)
l_{slot1}	4.4
l_{slot2}	4.9
$l_{\text{out_slot1}}$	6.5
$l_{\text{out_slot2}}$	8.05
d_{slot}	7.15
h_{slot}	3.5
$w_{\text{g_end}}$	4.02
$h_{\text{transition}}$	15
h_{cone}	8.77
A	22.5°



FIGURE 6: Novel SWAA prototype.

the array bandwidth, respectively. Table 2 summarizes the obtained results of the array main electromagnetic properties. Over the entire operating bandwidth, the proposed SWAA provides omnidirectional coverage in the azimuth plane with a measured gain from 12.49 to 14.71 dBi.

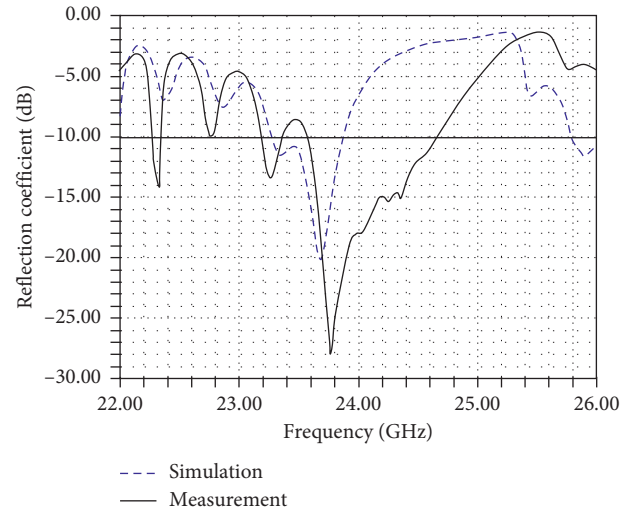


FIGURE 7: Reflection coefficient of the novel SWAA.

TABLE 2: Summary of the novel SWAA experimental results.

Frequency (GHz)	23.6	24.15	24.7
φ_{ab} ($^\circ$)	360	360	360
Gain ripple (dB)	2.5	2.7	2.7
θ_{ab} ($^\circ$)	5	5	6
SLL (dB)	-4.6	-5.18	-7.2
Gain (dBi)	14.71	12.49	13.14

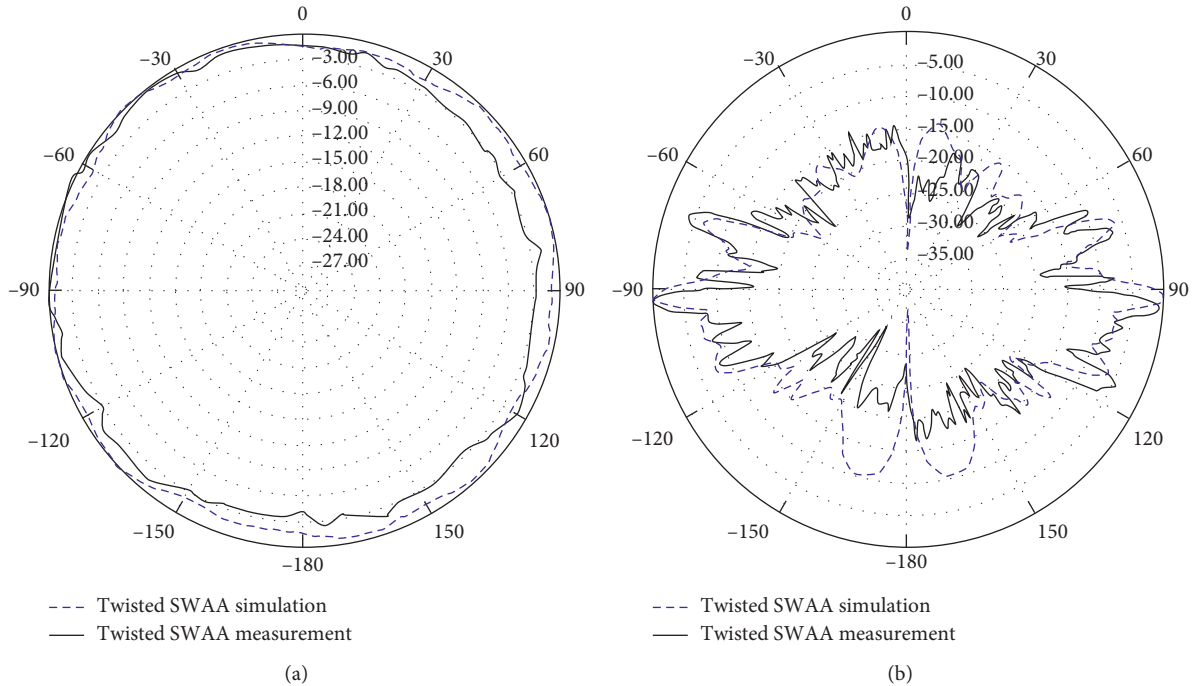


FIGURE 8: The novel SWAA radiation pattern characterization at 24.15 GHz. (a) Azimuth. (b) Elevation.

TABLE 3: Comparison among multiple omnidirectional antennas.

Reference	Manufacturing technology	Polarization	Gain (dBi)	Gain ripple (dB)	Operational frequency (GHz)	Bandwidth (GHz)
[25]	Printed	Vertical	1.8	0.5	5.7	1.07
[26]	Printed	Circular	2.4	1.5	2.45	0.245
[27]	Printed	Circular	2	0.6	2.6	0.52
Our work	SWAA	Vertical	12.49	2.7	24.15	1.09

Furthermore, its gain ripple has been kept below 3 dB for the entire bandwidth.

Figure 8 displays the SWAA radiation pattern characterization in the azimuth and elevation planes at 24.15 GHz. An excellent agreement between numerical simulation and measurement has been obtained for both planes. An unexpected gain degradation in the azimuth plane between 30° and -150° is observed, which can be explained by the wood holder used in the array characterization. Finally, by applying McDonald's equation for directivity estimation of omnidirectional antennas [23], we can compute a 13.11 dB of directivity at 24.15 GHz considering the measured bandwidth in the elevation plane, which means a radiation efficiency of 86%.

Finally, Table 3 presents a comparison of our approach with other state-of-the-art omnidirectional antennas published in literature [25–27]. Basically, our omnidirectional SWAA based on trapezoidal slots provides the following advantages: (i) enabling omnidirectional coverage in mm-waves; (ii) much higher gain compared with the printed omnidirectional antennas; (iii) bandwidth compatible with eMBB applications in mm-waves; (iv) high-power handling because of its manufacturing technology for base stations; and (v) linear polarization rather than circular polarization. The antenna presents itself as a potential solution for future

mobile systems, including some 5G femtocell indoor applications in the 24 GHz band.

4. Conclusions

We have successfully proposed and experimentally validated a slotted-waveguide antenna array with high-gain omnidirectional coverage, aimed at future indoor communication systems. The proposed antenna array is based on three new techniques proposed by our research group, namely, trapezoidal-shaped slots for generating a smooth impedance transition between waveguide inner part and air; groups of slots with distinct electrical lengths for creating multiple resonance frequencies; twisted distribution of slot groups along the array longitudinal axis, by means of an angular displacement. The joint application of the first two techniques resulted in a significant enhancement of three times in the array bandwidth when compared with the conventional SWAA design. Experimental results demonstrate 1.09 GHz bandwidth centered at 24.15 GHz, which corresponds to a fractional bandwidth of 4.52%. The third mentioned technique is able to significantly minimize the gain ripple in the azimuth plane and provide omnidirectional radiation pattern with gain up to 14.71 dBi, more than ten times higher than that of a conventional dipole applied

on indoor communication systems, which is approximately 2.15 dBi for omnidirectional coverage [23]. As a conclusion, the proposed twisted SWAA might be considered a viable solution for 5G eMBB communications, meeting the 3GPP-ETSI requirements for indoor communication, which requires up to 1 GHz bandwidth in the mm-wave frequency range [28]. Future works regard the deployment of the proposed array antenna in a 5G testbed, in conjunction with the previously developed GFDM-based 5G transceiver [29].

Data Availability

The data used to support the findings of this study are included in the article.

Conflicts of Interest

The authors declare that there are no conflicts of interest regarding the publication of this paper.

Acknowledgments

This work was partially supported by RNP, with resources from MCTIC, Grant no. 01250.075413/2018-04, under the Radiocommunication Reference Center (Centro de Referência em Radiocomunicações-CRR) project of the National Institute of Telecommunications (Instituto Nacional de Telecomunicações-Inatel), Brazil, and the Coordenação de Aperfeiçoamento de Pessoal de Nível Superior, Brasil (CAPES)-Finance Code 001. The authors from Brazil also thank the technical support from Keysight and financial support from CAPES, CNPq, and FAPEMIG. This work was also supported by the U.K. Engineering and Physical Sciences Research Council (Grant no. EP/P008402/2). The authors also would like to acknowledge the support of the University of Surrey 5GIC (<http://www.surrey.ac.uk/5gic>) members for this work.

References

- [1] CISCO Systems Inc., "Cisco 5G vision series: laying the foundation for new technologies, use cases, and business models," *1-19 White Paper*, CISCO Systems, San Jose, CA, USA, 2016.
- [2] M. Giordani, M. Mezzavilla, and M. Zorzi, "Initial access in 5G mmWave cellular networks," *IEEE Communications Magazine*, vol. 54, no. 11, pp. 40-47, 2016.
- [3] A. Osseiran, F. Boccardi, V. Braun et al., "Scenarios for 5G mobile and wireless communications: the vision of the METIS project," *IEEE Communications Magazine*, vol. 52, no. 5, pp. 26-35, 2014.
- [4] T. S. Rappaport, Shu Sun, R. Mayzus et al., "Millimeter wave mobile communications for 5G cellular: it will work!," *IEEE Access*, vol. 1, pp. 335-349, 2013.
- [5] S. Rangan, T. S. Rappaport, and E. Erkip, "Millimeter-wave cellular wireless networks: potentials and challenges," *Proceedings of the IEEE*, vol. 102, no. 3, pp. 366-385, 2014.
- [6] Y. Niu, Y. Li, D. Jin, L. Su, and A. V. Vasilakos, "A survey of millimeter wave communications (mmWave) for 5G: opportunities and challenges," *Wireless Networks*, vol. 21, no. 8, pp. 2657-2676, 2015.
- [7] S. Sun, T. Rappaport, R. Heath, A. Nix, and S. Rangan, "Mimo for millimeter-wave wireless communications: beamforming, spatial multiplexing, or both?," *IEEE Communications Magazine*, vol. 52, no. 12, pp. 110-121, 2014.
- [8] J. Jang, M. Chung, S. C. Hwang et al., "Smart small cell with hybrid beamforming for 5G: theoretical feasibility and prototype results," *IEEE Wireless Communications*, vol. 23, no. 6, pp. 124-131, 2016.
- [9] W. H. Watson, "Resonant slots," *Journal of the Institution of Electrical Engineers - Part IIIA: Radiolocation*, vol. 93, no. 4, pp. 747-777, 1946.
- [10] R. S. Elliot, "Basic considerations in the design of arrays," in *Proceedings of the European Microwave Conference*, pp. 561-565, Paris, France, September 1985.
- [11] J. Gulick, G. Stern, and R. Elliot, "The equivalent circuit of a rectangular-waveguide-fed longitudinal slot," in *Proceedings of the Antennas and Propagation Society International Symposium*, pp. 685-688, Philadelphia, PA, USA, June 1986.
- [12] S. R. Rengarajan, L. G. Josefsson, and R. S. Elliott, "Waveguide-fed slot antennas and arrays: a review," *Electromagnetics*, vol. 19, no. 1, pp. 3-22, 1999.
- [13] A. S. Cerqueira Jr., "A novel dual-polarization and dual-band slotted waveguide antenna array for dual-use radars," in *Proceedings of the European Conference on Antennas and Propagation (EuCAP)*, pp. 1-4, Davos, Switzerland, April 2016.
- [14] B. Pyne, P. R. Akbar, V. Ravindra, H. Saito, J. Hirokawa, and T. Fukami, "Slot-array antenna feeder network for spaceborne," *IEEE Transactions on Antennas and Propagation*, vol. 66, no. 7, pp. 3463-3474, 2018.
- [15] M. Ando, K. Sakurai, N. Goto, K. Arimura, and Y. Ito, "A radial line slot antenna for 12 GHz satellite TV reception," *IEEE Transactions on Antennas and Propagation*, vol. 33, no. 12, pp. 1347-1353, 1985.
- [16] S. Bernal, F. Vega, F. Roman, and A. Valero, "A high-gain, broad-wall slotted waveguide antenna array to be used as part of a narrowband high power microwaves system," in *Proceedings of the International Conference on Electromagnetics in Advanced Applications (ICEAA)*, pp. 618-621, Turin, Italy, September 2015.
- [17] D. Hotte, R. Siragusa, Y. Duroc, and S. Tedjini, "A concept of pressure sensor based on slotted waveguide antenna array for passive MMID sensor networks," *IEEE Sensors Journal*, vol. 16, no. 14, pp. 5583-5587, 2016.
- [18] A. S. Cerqueira Jr., I. F. da Costa, R. A. dos Santos, H. R. D. Filgueiras, and D. H. Spadoti, "Waveguide-based antenna arrays for 5G networks," *International Journal of Antennas and Propagation*, vol. 2018, Article ID 5472045, 10 pages, 2018.
- [19] I. F. da Costa, A. S. Cerqueira, D. H. Spadoti, L. G. da Silva, J. A. J. Ribeiro, and S. E. Barbin, "Optically controlled reconfigurable antenna array for mm-wave applications," *IEEE Antennas and Wireless Propagation Letters*, vol. 16, pp. 2142-2145, 2017.
- [20] H. R. D. Filgueiras, I. F. da Costa, S. A. Cerqueira, R. A. Santos, and J. R. Kelly, "Mechanically reconfigurable slotted-waveguide antenna array for 5G networks," in *Proceedings of the SBMO/IEEE MTT-S International Microwave and Optoelectronics Conference (IMOC)*, pp. 1-5, Aguas de Lindoia, Brazil, August 2017.
- [21] H. R. D. Filgueiras, I. F. da Costa, J. R. Kelly, A. S. Cerqueira Jr., and P. Xiao, "A novel approach for designing omnidirectional slotted-waveguide antenna arrays," in *Proceedings of*

- the International Conference on Electromagnetics in Advanced Applications (ICEAA)*, Cartagena, Colombia, September 2018.
- [22] H. R. D. Filgueiras and A. S. Cerqueira Jr., "Method for enhancing bandwidth in slot-based antennas and antenna arrays (in Portuguese)," *Patent BR10201801443*, Brazilian national Institute of industrial property (INPI), Brasilia, Brazil, 2018.
 - [23] C. A. Balanis, *Antenna Theory: Analysis and Design*, Wiley, Hoboken, NJ, USA, 4th edition, 2016.
 - [24] J. Tak, A. Kantemur, Y. Sharma, and H. Xin, "A 3-D-printed W-band slotted waveguide array antenna optimized using machine learning," *IEEE Antennas and Wireless Propagation Letters*, vol. 17, no. 11, pp. 2008–2012, 2018.
 - [25] A. Liu, L. Huang, and Y. Lu, "Wideband circular patch antenna with I-shaped structure for horizontal omnidirectional gain enhancement," *IET Microwaves, Antennas & Propagation*, vol. 13, no. 5, pp. 608–614, 2019.
 - [26] A. Wang, X. Li, X. Yi, L. Yang, J. Zhao, and A. Li, "Dual circularly polarised omnidirectional antenna," *IET Microwaves, Antennas & Propagation*, vol. 13, no. 6, pp. 870–873, 2019.
 - [27] L. Sun, Y. Li, Z. Zhang, and Z. Feng, "Compact Co-horizontally polarized full-duplex antenna with omnidirectional patterns," *IEEE Antennas and Wireless Propagation Letters*, vol. 18, no. 6, pp. 1154–1158, 2019.
 - [28] European Telecommunications Standards Institute (ETSI), "5G; study on scenarios and requirements for next generation access technologies," 3rd Generation Partnership Project (3GPP) Technical Report 3GPP TR 38.913 Version 17.2.0 Release 14, European Telecommunications Standards Institute (ETSI), Sophia Antipolis, France, 2017.
 - [29] R. M. Borges, T. R. R. Marins, and M. S. B. Cunha, "Integration of a GFDM-based 5G transceiver in a GPON using radio over fiber technology," *Journal of Lightwave Technology*, vol. 36, no. 19, pp. 4468–4477, 2018.

